Geophysical Research Letters

Supporting Information for

The origin of carbonate mud

Elizabeth J. Trower[1], Michael P. Lamb[2], and Woodward W. Fischer[2]

[1]Department of Geological Sciences, University of Colorado Boulder, Boulder, CO 80309; [2]Division of Geological and Planetary Sciences, California Institute of Technology, Pasadena, CA 91125; corresponding author: Elizabeth Trower (lizzy.trower@colorado.edu)

Contents of this file

Introduction

This supporting information document includes sections describing derivation of particle impact velocity (w_i) (Text S1), estimation of mud production fluxes for the Great Bahama Bank (Text S2), and settling velocity and advection length scale calculations (Text S3), a schematic of experimental set-up (Figure S1), an example grain size dataset illustrating identification of fragmentation products (Figure S2), sensitivity tests of model parameters k_v and k_m (Figure S3), SEM images of experimental and natural carbonate mud (Figure S3), a table of experimental parameters and results (Table S1), and a table of data for calculating k_m (Table S2).

Text S1. Particle impact velocity calculations

Particle impact velocity, w_i, is calculated as in Lamb et al., 2008 (cf. their eqn. 35):

$$w_i = \left[\int_{-w_s}^{6\sigma_w} (w' + w_s)^3 P dw'\right]^{1/3} \quad (1)$$

to account for gravitational settling and advection of particles by turbulence, where σ_w is the standard deviation of time averaged velocity fluctuations normal to the bed, approximated as $\sigma_w = u_*$ (Lamb et al., 2008) and P is the probability density function of velocity fluctuations (w'), defined as

$$P(w') = \frac{1}{\sqrt{2\pi}\sigma_w} e^{-\frac{w'^2}{2\sigma_w^2}} \quad (2)$$

The settling velocity, w_s, is assumed to be the terminal settling velocity and calculated using Dietrich (1982):

$$w_s = (RgvW_*)^{1/3} \quad (3)$$

where v is kinematic fluid viscosity (which was 1.3 x 10^{-6} m^2/s for our experiments) and W_* is dimensionless settling velocity. W_* is calculated as

$$W_* = R_3 10^{(R_1+R_2)} \quad (4)$$

R_1, R_2, and R_3 are empirically fitted equations that account for particle size, shape, and density, respectively:

$$R_1 = -3.76715 + 1.92944 \log D_* - 0.09815 (\log D_*)^2 - 0.00575 (\log D_*)^3 + 0.00056(\log D_*)^4 \quad (5)$$

$$R_2 = \left(\log\left(1 - \frac{1-\mathrm{CSF}}{0.85}\right)\right) - (1-\mathrm{CSF})^{2.3} \tanh(\log D_* - 4.6) + 0.3(0.5 - \mathrm{CSF})(1 - \mathrm{CSF})^2(\log D_* - 4.6) \quad (6)$$

$$R_3 = \left[0.65 - \left(\frac{\mathrm{CSF}}{2.83}\tanh(\log D_* - 4.6)\right)\right]^{\left(1+\frac{3.5-\mathrm{PS}}{2.5}\right)} \quad (7)$$

where $D_* = \frac{RgD^3}{\nu^2}$ is dimensionless particle size, CSF is the Corey shape factor (for ooids, we assume the particles are spherical and use CSF = 1; for skeletal sand, we use CSF = 0.8), and PS is the Powers roundness (for ooids, we assume a spherical particle and choose PS = 6; for skeletal sand, we use PS = 3.5).

As in the total-load bedrock erosion model (Lamb et al., 2008; Scheingross et al, 2014) and the ooid precipitation-abrasion model (Trower et al., 2017), the abrasion mud production model accounts for viscous damping of particle-bed impacts using a threshold particle Stokes number, $\mathrm{St}_c = \frac{Dw_i\rho_s}{9\nu\rho_f}$. The threshold used here is $\mathrm{St}_c = 10$, which, as in Trower et al. (2017), is required to match key experimental observations (measurable abrasion of medium-sand-sized grains near the threshold of suspension).

Text S2. Estimating mud production by abrasion for the Great Bahama Bank

Recently updated facies mapping of the Great Bahama Bank (Harris et al., 2015) were combined with model mud production rates to estimate the potential contributions of abrasion from either a single large storm or a typical year of fair-weather conditions to the Great Bahama Bank mud budget calculated by Robbins et al. (1997). The area of the Great Bahama Bank is 3.3 x 10^9 m^2 (Robbins et al., 1997). For a large hurricane, we assume that all grainy material on the platform, which covers 65% of the platform area (Harris et al., 2015), can be transported in suspension or washload for a 24-hour period, which corresponds to a mud production rate on the order of 10^4 $g/m^2/yr$, or ~27 $g/m^2/day$. This suggests that abrasion during a hurricane could generate ~6 x 10^{10} g of carbonate mud, or roughly 4% of the annual mud production of 1.4 x 10^{12} g estimated by Robbins et al. (1997). For fair weather abrasion, we use a more conservative area—the 45% of the Great Bahama Bank characterized by grainstone facies (Harris et al., 2015), which correspond to current-active zones. Using our slowest experimental mud production rate, ~$10^{2.5}$ $g/m^2/yr$, we calculate that abrasion could produce ~5 x 10^{11} g of carbonate mud, or 36% of the annual mud budget. These calculations suggest that abrasion of grainy sediment during both fair weather conditions and storms are likely to make a substantial contribution to mud production on the Great Bahama Bank.

Text S3. Calculating advection length scales for individual mud particles and floccules

Settling velocities for carbonate sand ($w_{s\text{-}sand}$) were calculated following Dietrich (1982) using Corey shape factor (CSF) = 1 for a spherical ooid and CSF = 0.8 for a carbonate sand grain, and Powers roundness (PS) = 6 for a spherical ooid and PS = 3.5 for a carbonate sand grain (see Equations 3-7 in Text S1). Settling velocities for single aragonite needles ($w_{s\text{-}mud}$) were calculated following Stokes Law for a cylindrical particle, incorporating our observations of particle dimension:

$$w_{s-mud} = \frac{1}{12}\frac{Rg}{\nu}\frac{V_p D_{int}}{A_\perp} \quad (8)$$

where D_{int} is intermediate axis dimension and $A_\perp$ is the particle cross-sectional area perpendicular to flow.

Flocculation of individual mud particles into larger floccules can increase settling velocities. We used observations of the size of floccules composed of mud-sized carbonate particles (Schieber et al., 2013) to estimate a maximum average floccule size of 50 μm under transport conditions where carbonate sand is above the threshold of motion. We used an empirical relationship between floccule size and density (Fennessy et al., 1994) to estimate floccule density and calculated floccule settling velocity ($w_{s\text{-}floc}$) following Dietrich (1982).

Advection length scale of settling sediment (Ganti et al., 2014) (l_a) is a function of flow velocity (u), average settling height (h_s), and particle setting velocity (w_s):

$$l_a = \frac{uh_s}{w_s} \quad (9)$$

Typical settling heights for rippled sand in oscillatory flow scale with ripple heights (van der Werf et al., 2007): $h_{s\text{-}sand} \approx$ 1-5 cm. In contrast, mud particles produced by abrasion of sand will be transported as washload by initial flow conditions and prior to flocculation, so mud particle settling heights should scale with water depth: $h_{s\text{-}mud}$ = 1-5 m. The ratio of advection length scales (R_{al}) of mud or flocculated mud can therefore be calculated as:

$$R_{al,mud:sand} = \frac{h_{s-mud}w_{s-sand}}{h_{s-sand}w_{s-mud}} \quad (10)$$

$$R_{al,floc:sand} = \frac{h_{s-mud}w_{s-sand}}{h_{s-sand}w_{s-floc}} \quad (11)$$

Although the ratio of settling heights ($h_{s\text{-}mud}/h_{s\text{-}sand}$) will vary depending on a variety of parameters, a conservative estimate with $h_{s\text{-}sand}$ = 5 cm and $h_{s\text{-}mud}$ = 1 m suggests that $R_{al,floc:sand} >$ 1000: smaller sand settling heights, larger mud settling heights, smaller flocs, and a lesser degree of flocculation all predict larger $R_{al,mud:sand}$ by up to 3 orders of magnitude. Advection length scales for rippled carbonate sand in oscillatory flow are on the order of a few centimeters to tens of centimeters, depending on flow velocity, which indicates that advection length scales for mud produced by abrasion should range from tens of meters to tens of kilometers. Considering that this material will initially be in the washload, estimates at the longer end of this range are more accurate because currents within tens of meters of the original location are likely too strong for mud to flocculate and/or settle to the bed.

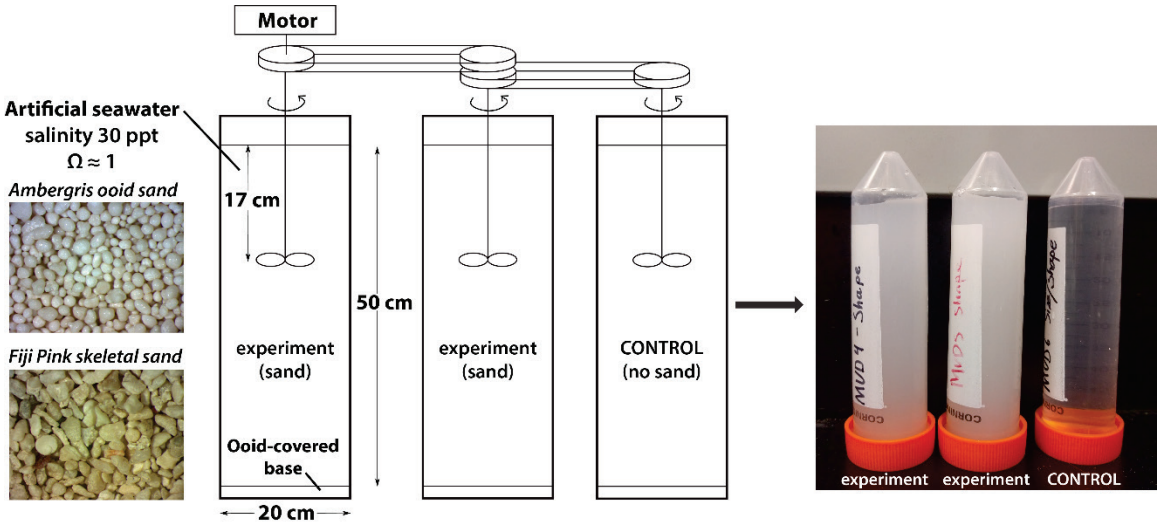

Figure S1. Schematic of abrasion mill experimental set-up, including examples of water column samples for mud mass determination.

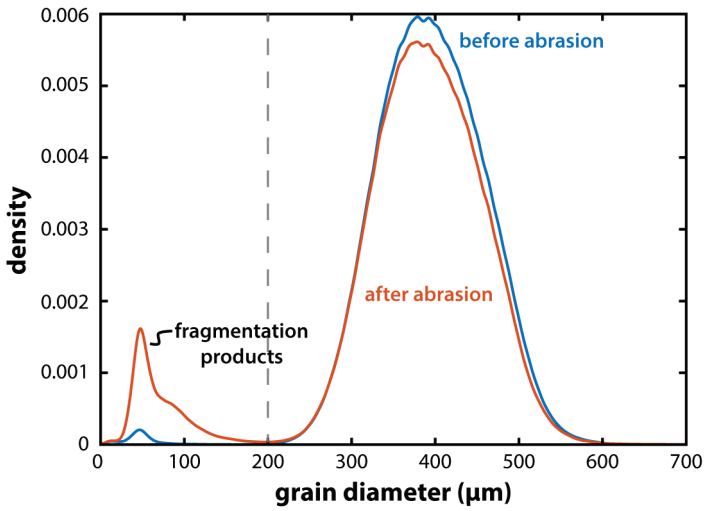

Figure S2. Kernel-smoothing probability density estimates for grain size data from trial MUD1. This example illustrates the overall decrease in grain size of the carbonate sand and the production of very-fine-sand to silt-sized material via fragmentation. To determine the proportion of sand abrasion partitioned as mud production, we subtracted the increase in volume of very fine grains (for this sample, those with diameters <200 μm, indicated by dashed grey line) from the decrease in volume of the primary sand fraction. These estimates are given in Table S2.

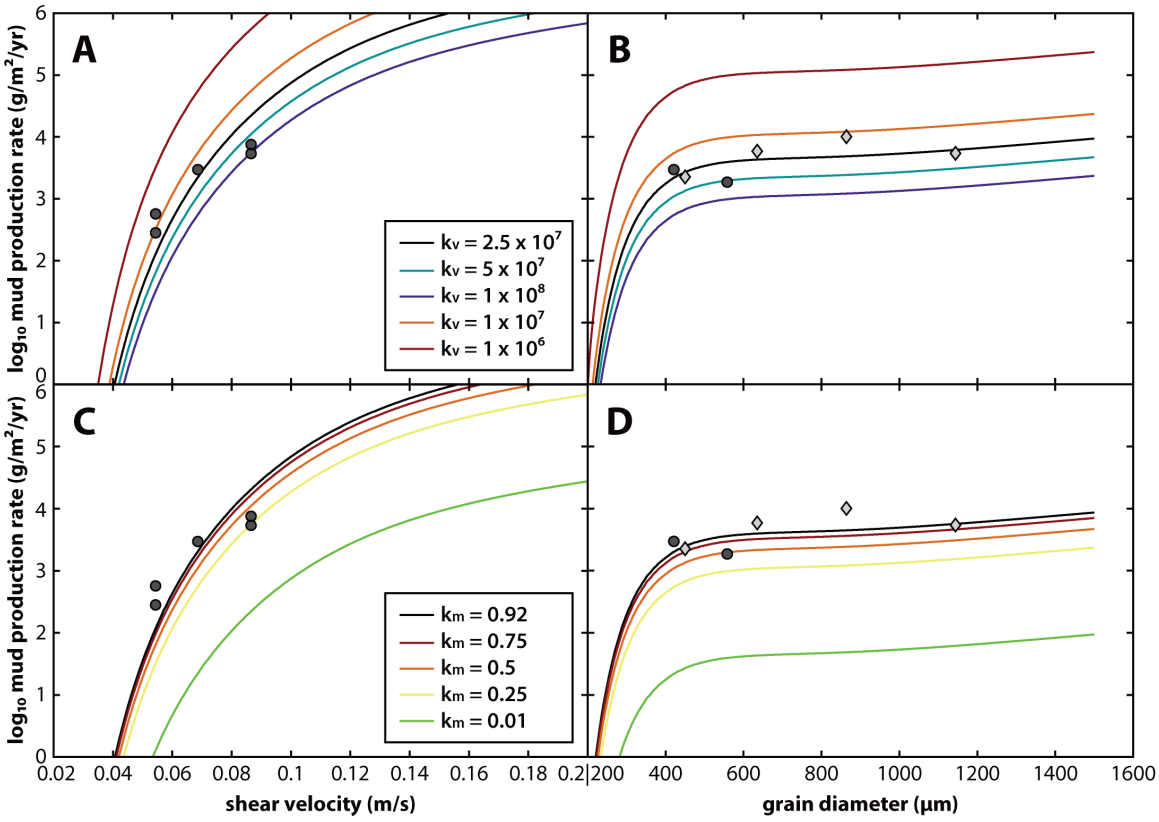

Figure S3. Sensitivity tests of k_v (A, B) and k_m (C, D), both of which were calibrated using experimental data: k_v was calibrated to optimize model fit to experimental rate data and k_m was set to experimentally determined fragmentation rate (Table S2).

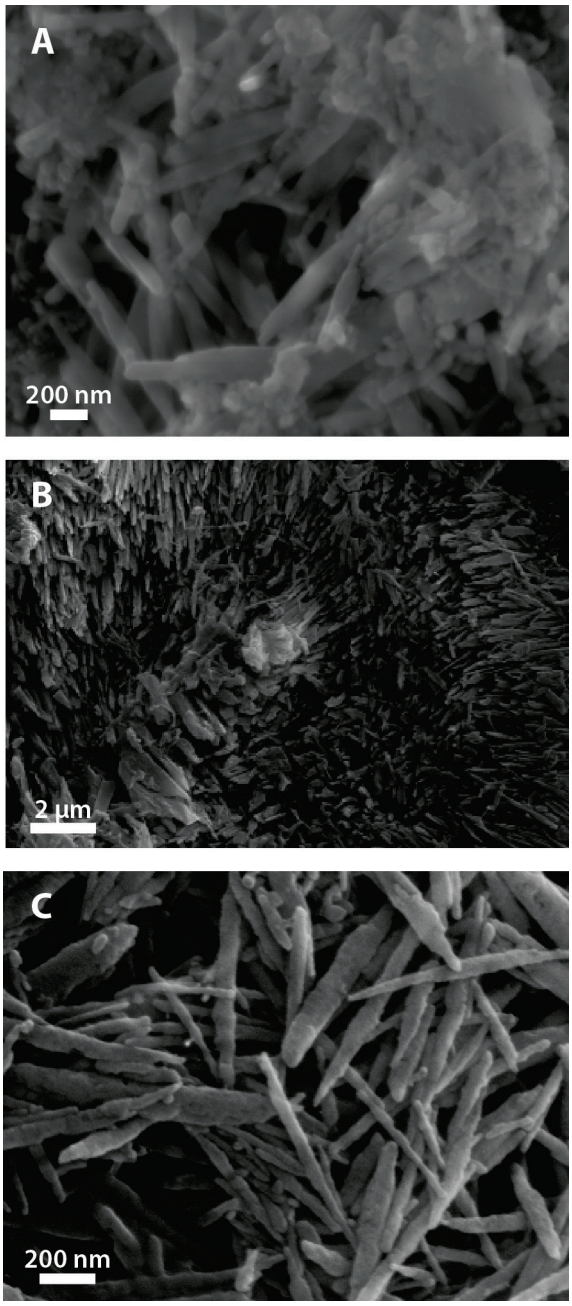

Figure S4. SEM images comparing aragonite mud produced via abrasion mill experiment (A), the cortical texture of a representative ooid from the population used for experiments (B), and mud filtered from seawater collected at the same field site as these ooids (C).

Run #	Trial	Material	Duration (hr)	Initial D_{50} (μm)	$u*$ (m/s)	Mud production rate ($mg/m^2/hr$)		log_{10} (average mud production rate)
						Grain size	Mud mass	
1	MUD1	Ooid	193.6	421	0.069	9.0	11.2	3.45
1	MUD2	Ooid	193.6	558	0.069	6.2	6.5	3.25
1	MUD3	Control	193.6	N/A	0.069	N/A	n.d.	N/A
2	MUD4	Skeletal	335.5	635	0.069	25.0	15.5	3.75
2	MUD5	Skeletal	335.5	864	0.069	40.6	28.7	3.99
2	MUD6	Control	335.5	N/A	0.069	N/A	n.d.	N/A
3	MUD7	Skeletal	334.3	1144	0.069	23.4	14.1	3.72
3	MUD8	Skeletal	334.3	450	0.069	13.8	2.1	3.35
3	MUD9	Control	334.3	N/A	0.069	N/A	n.d.	N/A
4	MUD10	Ooid	644.8	426	0.054	4.1	n.d.	2.76
4	MUD11	Ooid	644.8	420	0.054	2.0	n.d.	2.45
4	MUD12	Control	644.8	N/A	0.054	N/A	n.d.	N/A
5	MUD13	Ooid	197.0	410	0.087	21.0	30.0	3.85
5	MUD14	Ooid	197.0	407	0.087	18.3	18.5	3.71
5	MUD15	Control	197.0	N/A	0.087	N/A	n.d.	N/A
6	MUD19	Skeletal	0.89	856	0.094	115.3	74.4	4.42
6	MUD20	Skeletal	0.89	860	0.094	99.1	57.8	4.34
6	MUD21	Control	0.89	N/A	0.094	N/A	n.d.	N/A

n.d. – not detected: mud mass was below measurable threshold
Variation in log rates between duplicate trials is 6-21%.

Table S1. Experimental parameters and results for abrasion mill experiments

Run #	Trial	Material	Total abrasion rate (mm^3/hr)[a]	Fragmentation abrasion rate (mm^3/hr)[b]	Mud production rate (mm^3/hr)	k_m[c]
1	MUD1	Ooid	3.36	0.21	3.14	0.94
1	MUD2	Ooid	2.64	0.49	2.16	0.82
2	MUD4	Skeletal	9.06	0.28	8.78	0.97
2	MUD5	Skeletal	14.5	0.24	14.2	0.98
3	MUD7	Skeletal	10.3	2.04	8.22	0.80
3	MUD8	Skeletal	5.08	0.23	4.85	0.95
4	MUD10	Ooid	1.47	0.034	1.43	0.98
4	MUD11	Ooid	0.79	0.080	0.71	0.90
5	MUD13	Ooid	7.90	0.52	7.38	0.93
5	MUD14	Ooid	7.62	1.21	6.41	0.84
6	MUD19	Skeletal	41.2	0.76	40.5	0.98
6	MUD20	Skeletal	35.5	0.72	34.8	0.98

[a]Total abrasion rate is estimated using the change in mean grain volumes between measurements before and after each experiment.
[b]Fragmentation abrasion rate is estimated by calculating the total volume of grains whose sizes fall in the secondary peak of the post-experiment grain size distribution for each trial. These distributions are bimodal, with one large peak similar to the distribution prior to the experiment and a subpeak at sizes finer than the pre-experiment distribution. This subpeak represents new grains produced via fragmentation. The cutoff is chosen as the minimum between these two peaks.
[c]k_m is estimated as the proportion of the total abrasion rate that cannot be accounted for by the fragmentation abrasion rate.

Table S2. Data for calculating fragmentation rate and k_m